Self-Assembled Nanofold Network Formation on Layered Crystal Surfaces during Metal Intercalation

E. Spiecker,[1,2,*] A. K. Schmid,[1] A. M. Minor,[1] U. Dahmen,[1] S. Hollensteiner,[2] and W. Jäger[2]

[1]*National Center for Electron Microscopy, Lawrence Berkeley National Laboratory, Berkeley, California 94720, USA*

[2]*Mikrostrukturanalytik, Technische Fakultät, Christian-Albrechts-Universität zu Kiel, Kaiserstraße 2, 24143 Kiel, Germany*

(Received 6 July 2005; published 27 February 2006)

We study the formation of planar network nanostructures, which develop during metal deposition on initially smooth surfaces of layered compounds. Using *in situ* low-energy electron microscopy for dynamic observation and high-resolution transmission electron microscopy for structure analysis, we have observed the rapid formation of hexagonal networks of linear "nanofolds" with prismatic cavities on top of layered VSe_2 crystals. Their formation results from relaxation of compressive strains which build up during Cu intercalation into a thin surface layer.

DOI: 10.1103/PhysRevLett.96.086401 PACS numbers: 61.46.−w, 68.37.Lp, 68.37.Nq, 81.15.Ef

Layered crystal structures possess unique properties which enable the manufacturing of nanostructures. The weak van der Waals-type interlayer bonding in layered crystals, like graphite or the transition metal dichalcogenides (TMDC), allow the layers to be easily separated or shifted relative to each other [1–3]. In contrast, the individual layers are rather stable due to strong intralayer bonds. Thus the layers can be bent or folded on a nanometer scale without destroying their crystal structure, as shown also by the structural integrity of nanotubes composed of such layered materials [4,5]. While these nanostructures tend to form as isolated units, there is increasing interest in arranging them in regular networks with well-defined nodes. Indeed, possibilities to create branched nanotubes are a topic of great current interest [6–8].

Recently, a remarkable phenomenon of self-assembled nanostructure network formation on top of layered TMDC crystals has been reported [9,10]: Induced by vacuum deposition of Rb (Cu) onto cleaved surfaces of $TiTe_2$ (VSe_2) linear nanostructures with lateral dimensions of the order of 10 nm form spontaneously and arrange themselves in hexagonal networks with mesh sizes of the order of 1 μm. However, the interpretation of this phenomenon remained controversial. First, such nanostructures have been interpreted as metal nanowires formed within cracks in the layered crystal surface [9–12]. In this interpretation, the possibility of a chemical interaction of the metal and the layered crystal was not taken into account. More recently, the model invoking metal nanowires was questioned when photoelectron spectroscopy (PES) studies of $TiTe_2$ surfaces after Rb deposition [13,14] and transmission electron microscopy (TEM) investigations of VSe_2 surfaces after Cu deposition [15,16] indicated that the metal atoms intercalate into the layered crystal. Based on plan-view TEM it was proposed that the nanostructures are folds of the layered crystal surface rather than metal nanowires [15].

To solve this puzzle, we used state-of-the-art techniques, including *in situ* low-energy electron microscopy (LEEM), cross sectioning by focused ion beam (FIB) thinning, and high-resolution transmission electron microscopy (HRTEM), to take a new look at the Cu/VSe_2 system. Our results prove that the networks are nanoscale folding patterns, which form as a result of metal intercalation and strain relief, while we find no evidence for the condensation of the metal into nanowire networks.

In our experiments we used VSe_2 layered crystals prepared by chemical vapor transport. Such VSe_2 crystals consist of Se-V-Se layer sandwiches with V atoms octahedrally coordinated by Se atoms [1*T* structure cf. Fig. 4(a)]. Clean (0001) surfaces were obtained by cleavage under high vacuum conditions immediately before transfer into the ultrahigh vacuum chamber of the low-energy electron microscope. Cu was deposited from a Knudsen cell onto the VSe_2 surfaces at ambient temperature with a nominal rate of 0.155 nm/min while surface areas of $\sim$7 μm diameter were imaged by *in situ* LEEM at a rate of 1 frame/s. After deposition, the surface structures were studied by scanning electron microscopy (SEM) and by TEM in plan-view and cross-section geometry. For plan-view TEM thin foils were cleaved from the VSe_2 crystal surface with a razor blade technique. A FIB preparation method which avoids deposition of a protective layer was newly developed and applied to prepare cross sections for high-resolution TEM investigations. The TEM investigations were carried out with a JEOL 3010 microscope and a Philips CM300FEG-UT microscope.

A typical network of nanostructures formed on a flat VSe_2 surface upon Cu deposition for 22 min is shown by the SEM image Fig. 1(a). The mesh size of the network ranges between 400 and 800 nm. The network comprises mainly triple junctions where three nanostructures meet at 120°. The hexagonal pattern reflects the symmetry of the VSe_2 substrate crystal and is indicative of the crystallographic nature of the formation process. The TEM bright-field image Fig. 1(b) shows an individual nanostructure at the edge of a plan-view sample. The feature is $\sim$30 nm wide and shows a separation into two characteristic, par-

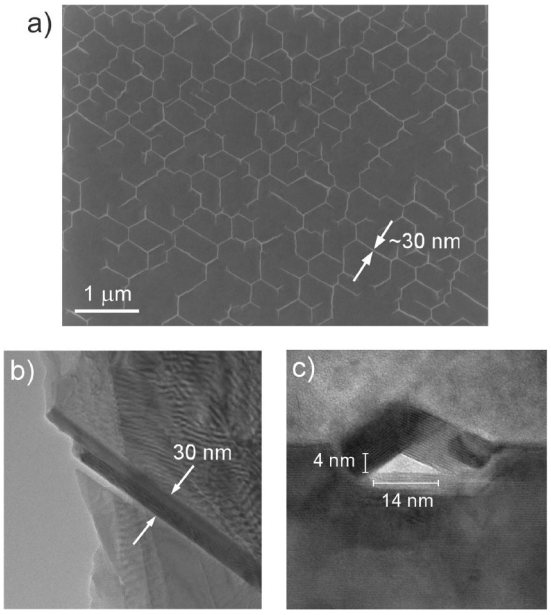

FIG. 1. (a) SEM image of a self-assembled hexagonal network of nanofolds formed on a VSe_2 surface by Cu deposition. (b) Plan-view TEM image of an individual nanofold showing the characteristic separation into two parallel strands. (c) HRTEM image of a FIB-prepared cross section showing a nanofold with a rooflike structure and a prismatic cavity.

allel strands. The HRTEM image of the cross section reproduced in Fig. 1(c) shows very clearly that the structures are nanosized surface folds (''nanofolds'') covering prismatic cavities. In total the imaged nanofold is about 25 nm wide. The cavity shows a triangular cross section and is covered by crystalline tiles of about 10 nm thickness. The apex angle of the cavity is close to 120°, and the roof segments display relatively sharp interfaces. It appears that the fold was formed by delamination of the topmost layers and lateral displacement of layered material towards the delaminated region.

To capture the dynamics of the formation of the nanofold networks, we used LEEM to image the VSe_2 surface *in situ* during continuous Cu deposition. We find that the nanofold networks form abruptly within a short time interval (Fig. 2). During the first 781 seconds of Cu deposition, corresponding to a nominal coverage of ~2 nm, the surface contrast remains virtually unchanged [Fig. 2(a)]. The surface appears largely flat, except for the few surface steps (dark lines) and a curved defect (near the image center). The subsequent image, taken 1 s later [Fig. 2(b)], shows that the surface is now completely covered with a network of surface nanofolds. The sudden appearance of the network within ≤ 1 s shows that the velocity of fold propagation must be at least 7 μm/s. This fast dynamics indicates that the fold formation is the result of the sudden relaxation of supercitical surface layer strain. During further deposition the nanofold network turned out to be stable until, at a considerably later time (>920 s), a few more folds form and link up with the existing network.

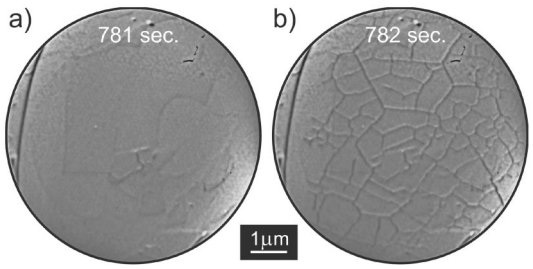

FIG. 2. Two subsequent images out of a sequence of >2500 *in situ* LEEM images showing the rapid formation (≤ 1 s) of a nanofold network on a VSe_2 surface during continuous Cu deposition.

The results of plan-view TEM analyses, summarized in Fig. 3, support our interpretation of the nanofold network formation as result of Cu intercalation. The bright-field image Fig. 3(a) shows a typical network region of a sample that had been exposed to the Cu vapor beam for 22 min. The diffraction pattern is inserted such that the crystallographic orientations are correctly reproduced. Reflections of type {10-10} and {11-20} are marked by small and large hexagons, respectively. The nanofolds of the network preferentially follow ⟨11-20⟩ directions. Folds that appear to align along ⟨10-10⟩ show undulations or break into short

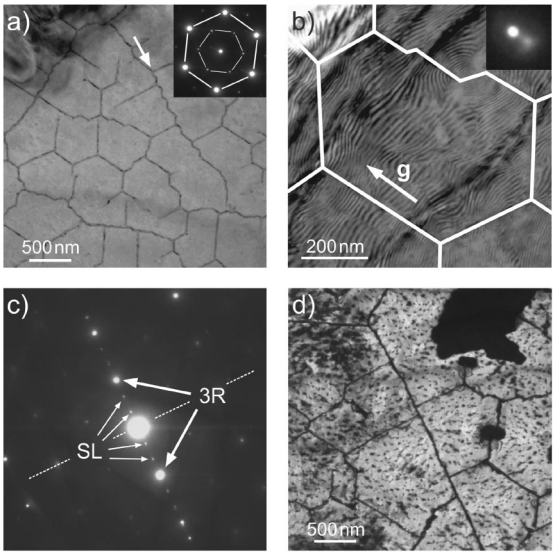

FIG. 3. Results of plan-view TEM investigations: (a) Bright-field (BF) image of a nanofold network and [0001] zone-axis diffraction pattern (inset) showing that the nanofolds are aligned along low index crystallographic directions. (b) BF image of network mesh (marked by bold white lines) with moiré fringes and corresponding reflection splitting (inset) indicating the presence of a surface layer with expanded lattice. (c) Diffraction from the surface layer which shows $3R$ polytype and superlattice (SL) spots indicating an ordered arrangement of the Cu intercalation atoms in the $3R - VSe_2$ layer stacking. (d) Dark-field image formed with a $3R$ reflection showing the almost contiguous surface layer (bright areas) separated by the nanofold network (dark lines).

segments along ⟨11-20⟩ (see arrow). A detailed inspection of the diffraction pattern reveals that the reflections of type {11-20} are actually split into two separate reflections [Fig. 3(b), inset]. The weaker reflection stems from a thin surface layer and has a shorter diffraction vector than the stronger substrate reflection, indicating a lattice expansion of the thin surface layer of ~1.4%. Correspondingly, bright-field micrographs taken under two-beam condition for a {11-20} reflection show moiré fringes, which extend preferentially perpendicular to the excited diffraction vector **g** [Fig. 3(b)]. TEM images taken under two-beam diffraction conditions for {10-10} reflections do not show any moiré fringes, indicating a $1T \rightarrow 3R$ polytype transformation in the thin surface layer. In the $3R$ polytype, the V atoms are in trigonal prismatic coordination with Se atoms, in contrast to the octahedral coordination in the $1T$ polytype, and one period along the c axis comprises three Se-V-Se sandwich layers (Fig. 4). Reflections of type {10-10} are forbidden in the $3R$ structure [17]. Figure 3(c) shows a diffraction pattern in which $3R$ reflections of the thin surface layer have been brought into diffraction condition by tilting the crystal lattice through ~18° from its ⟨0001⟩ surface orientation [cf. Fig. 4(b)]. The diffraction pattern in Fig. 3(c) also clearly reveals additional superstructure reflections (marked SL) at 1/3 of the distance between $3R$ reflections. The $1T \rightarrow 3R$ polytype transformation and the occurrence of commensurate superlattice reflections are indicative of the formation of a thin layer of a Cu/VSe_2 intercalation phase in which the Cu atoms show an ordered arrangement in the van der Waals gaps of a $3R$-VSe_2 layer stacking. Figure 3(d) shows a TEM dark-field image formed with a $3R$ reflection of the intercalation layer. The layer appears bright and covers nearly the entire surface. The nanofolds, representing tilted crystal regions, appear as dark lines.

$1T \rightarrow 3R$ polytype transformations have been reported also for electrochemical intercalation of Cu into bulk VSe_2 [18] and for vacuum intercalation of K into VSe_2 [19] and of Cs into TiS_2 [17]. X-ray diffraction measurements of bulk $3R$-VSe_2/Cu intercalation compounds show lattice expansions in the range 0.9%…1.6% for the basal plane relative to VSe_2 [18], in line with our observations.

Our experimental results can be explained consistently within the model sketched in Fig. 5: The impinging metal atoms (a) diffuse into the uppermost layers of the layered crystal and form an intercalation phase (b). This phase transformation is accompanied by a lattice expansion, which is constrained by the rigid substrate, leading to build up of compressive biaxial strain and stress in the intercalation layer. Beyond a critical layer thickness nanofolds form, propagate, and branch with high velocity across the surface, thereby forming the networks (c). The layer strain in the mesh regions relaxes by the lateral displacement of layer material towards the fold regions (arrows). This process is intimately connected to the excellent slip properties of layered crystals for the basal plane.

A consistency check of the relationship between in-plane strain, fold geometry, and mesh dimension supports the proposed mechanism. We assume that each individual nanofold segment contributes to the relaxation of layer strain only perpendicular to the fold axis. Furthermore, we assume a typical lateral fold size L of 25 nm and a triangular fold geometry with a roof angle of 120° (cf. Fig. 1). Then the amount of layered material shifted from adjacent regions towards the fold approximately corre-

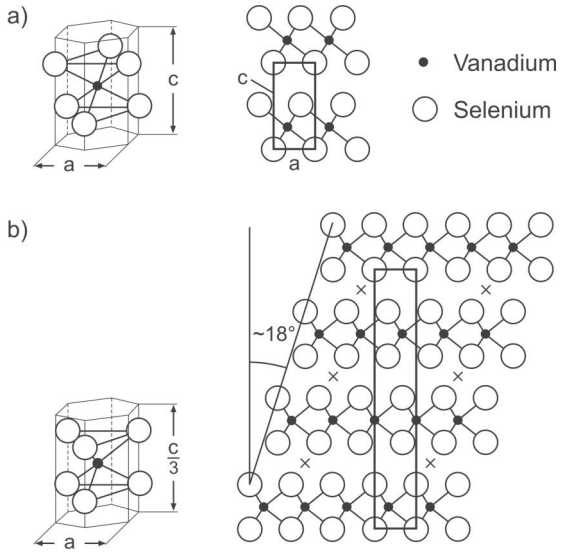

FIG. 4. (a) $1T$ structure of bulk VSe_2. (b) $3R$ structure of VSe_2 in the copper intercalation phase. The crosses in the van der Waals gaps mark possible positions for intercalated Cu atoms consistent with the superlattice reflections (SL) in the experimental diffraction pattern [Fig. 3(c)].

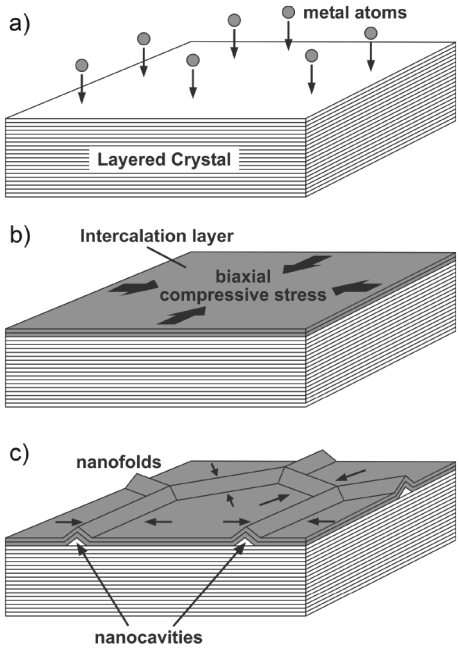

FIG. 5. Formation of networks of nanofolds with cavities upon vacuum metal intercalation into layered crystal surfaces during continuous metal deposition. For details, see text.

sponds to a stripe of width $L(1/\cos 30° - 1) \sim 4$ nm. To completely accommodate a 1.4% uniaxial strain, a parallel array of nanofolds of width $L = 25$ nm would need a spacing $d = 4\ \text{nm}/0.014 \sim 300$ nm, a value of the same order of magnitude as the observed mesh dimension.

The proposed mechanism is furthermore supported by an estimate of the critical intercalation-layer thickness for fold formation, h_c. In order to form a fold pattern, the elastic strain energy stored in the layer has to be at least as high as the energy required to delaminate the layers beneath the folds. The elastic strain energy per unit surface area is given by $E_{\text{el}} = \varepsilon^2 Y h$ with ε, Y, and h denoting the biaxial layer strain ($\sim$1.4%), the Young's modulus for biaxial strain of the intercalation layer, and the layer thickness, respectively. The energy for layer delamination is given by $E_{\text{del}} = fnE_0$ with f, n and E_0 denoting the fraction of the layer area delaminated from the substrate, the area density of interface atoms (10.32 nm^{-2}), and the binding energy per atom, respectively. From the fold size and the network dimension f can be estimated to amount to $\sim$5%. The modulus is not known for Cu-intercalated VSe_2, but $Y = 100$ GPa is a reasonable guess for a single crystalline layer. For the binding energy we estimate $E_0 = 60$ meV, which corresponds to the value calculated by density functional theory for the dichalcogenide MoS_2 [3]. By equating the energies E_{el} and E_{del} we find that the critical layer thickness for fold pattern formation is small, of the order of $h_c \sim 0.25$ nm. The observed thickness of the delaminated layer in the nanofolds [Fig. 1(b)] is substantially larger than this estimated critical thickness, which supports the interpretation that the fold pattern formation is the result of the relaxation of supercritical surface layer strain.

Networks of folds with considerably larger dimension—typically in the micrometer or millimeter range—are well known for compressively strained thin films or coatings, which are only weakly bonded to a substrate, e.g., for diamondlike carbon films on glass [20] or for metal films on polymers [21]. Current models attempting to describe the formation of such fold patterns by buckling-driven delamination [22,23] are inadequate to describe our observation of nanofold pattern formation on layered crystal surfaces, since they do not account for slip of film material on the substrate. In our case the interface between the intercalation layer and the VSe_2 substrate is a preferred slip plane allowing for efficient lateral transport of layer material towards the fold region. These processes enable a uniform relaxation of layer stress in the mesh regions of the fold network.

In summary, our results clearly show that the nanostructure networks on VSe_2 induced by Cu deposition consist of nanosized surface folds which form as result of the lattice expansion of a thin intercalation layer. These results are not consistent with networks of metal nanowires, as proposed earlier [9–12]. The formation of such nanofolds with linear cavities is a phenomenon that may be transferred to other layered crystals. The main requirement for the nanofold formation is selective lattice expansion of the uppermost surface layers, achieved in the present case by metal intercalation upon vacuum deposition. The interconnected planar network of prismatic cavities within the nanofolds may have technological applications. Similar to the filling of nanotubes with different materials [24,25], filling of the cavities may be used to fabricate nanowire arrays. The observed branching with crystallographically controlled angles offers additional possibilities for new types of interconnected nanoscale structures.

We thank L. Kipp from the University of Kiel for providing the VSe_2 crystals. This work was supported by the U.S. Department of Energy under Contract No. DE-ACO2-O5CH11231, by the German Science Foundation (DFG) under Contract No. FOR 353/1-2, and by the Alexander von Humboldt Foundation (E. S., Feodor Lynen Program).

*To whom correspondence should be addressed.
Electronic address: es@tf.uni-kiel.de

[1] D. E. Soule and C. W. Nezbeda, J. Appl. Phys. **39**, 5122 (1968).
[2] A. M. Fennimore *et al.*, Nature (London) **424**, 408 (2003).
[3] H. Rydberg *et al.*, Phys. Rev. Lett. **91**, 126402 (2003).
[4] R. H. Baughman, A. A. Zakhidov, and W. A. de Heer, Science **297**, 787 (2002).
[5] R. Tenne and C. N. R. Rao, Phil. Trans. R. Soc. A **362**, 2099 (2004).
[6] M. Terrones *et al.*, Phys. Rev. Lett. **89**, 075505 (2002).
[7] J.-M. Ting and C.-C. Chang, Appl. Phys. Lett. **80**, 324 (2002).
[8] R. H. Bandaru *et al.*, Nat. Mater. **4**, 663 (2005).
[9] R. Adelung *et al.*, Phys. Rev. Lett. **86**, 1303 (2001).
[10] R. Adelung *et al.*, Adv. Mater. **14**, 1056 (2002).
[11] R. Adelung, W. Hartung, and F. Ernst, Acta Mater. **50**, 4925 (2002).
[12] R. Adelung *et al.*, Nat. Mater. **3**, 375 (2004).
[13] S. E. Stoltz, H. I. Starnberg, and L. J. Holleboom, Europhys. Lett. **64**, 816 (2003).
[14] S. E. Stoltz, H. I. Starnberg, and L. J. Holleboom, Phys. Rev. B **71**, 125403 (2005).
[15] E. Spiecker *et al.*, Microsc. Microanal. **11**, 456 (2005).
[16] S. Hollensteiner, E. Spiecker, and W. Jäger, Appl. Surf. Sci. **241**, 49 (2005).
[17] C. Remškar, A. Popovič, and H. I. Starnberg, Surf. Sci. **430**, 199 (1999).
[18] K. Sollmann, Ph.D. thesis, Technical University of Berlin, 1995.
[19] I. I. Pronin *et al.*, Surf. Sci. **461**, 137 (2000).
[20] S. B. Iyer, K. S. Harshavardkan, and V. Kumar, Thin Solid Films **256**, 94 (1995).
[21] A. Pundt *et al.*, Acta Mater. **52**, 1579 (2004).
[22] G. Gioia and M. Ortiz, Adv. Appl. Mech. **33**, 119 (1997).
[23] B. Audoly, Phys. Rev. Lett. **83**, 4124 (1999).
[24] P. M. Ajayan and S. Iijima, Nature (London) **361**, 333 (1993).
[25] M. Monthioux, Carbon **40**, 1809 (2002).